ELSEVIER_APT_1739

Original Research Paper

Influence of the reduction strategy in the synthesis of reduced graphene oxide

M.P. Lavin-Lopez[a,*]
pradolavin@graphenano.com

A. Paton-Carrero[b]

L. Sanchez-Silva[b]

J.L. Valverde[b]

A. Romero[b]

[a]Graphenano S.L., Calle Pablo Casals 13, 30510 Yecla, Murcia, Spain

[b]University of Castilla-La Mancha, Department of Chemical Engineering, Avenida Camilo Jose Cela 12, 13071 Ciudad Real, Spain

*Corresponding author.

Abstract

In this work, a comparative study of the different graphene oxide reduction strategies to produce reduced graphene oxide are discussed. Firstly, the optimization of the well-known oxidation route reported in literature (Improved Hummers Method) to obtain graphite oxide was carried out. Subsequently, different sets of reduced graphene oxide powders were synthesized through three different reduction routes: chemical, thermal and multiphase methods in order to obtain the most effective reduction strategy. Samples were analyzed by Raman spectroscopy, SEM, FTIR, elemental analysis, X-ray Diffraction and TGA. It was demonstrated that multiphase reduction method, e.g. combination of more than one reduction route, specifically, thermal and chemical ones, allowed to enhance the effectiveness for the removal of the oxygen functional groups. A mild thermal treatment followed by a chemical reduction of graphene oxide using ascorbic acid as reducing agent, showed that the 47% of oxygen functional groups was reduced. This manuscript demonstrates that the amount of oxygen functional groups in the reduced graphene oxide structure is highly dependent on the reduction strategy. These amount of oxygen functional groups could directly affect the use of reduced graphene oxide in the different potential applications proposed in bibliography.

Keywords: Reduced graphene oxide; Removal of oxygen functional groups; Chemical reduction; Thermal reduction; Multiphase reduction

1 Introduction

Graphene is a two-dimensional (2D) carbon allotrope with a honey-comb lattice shape in which each carbon atom forms one vertex [1]. Since its discovery in 2004, graphene has been attracted the attention of researchers due to its extraordinary properties and its potential applications [2]. The large variety of methods to synthesize graphene, such as mechanical exfoliation process and cleavage [3], chemical vapor deposition (CVD) [4] or chemical reduction of graphene oxide [5], can be grouped in two different approaches: Bottom-Up or Top Down. Bottom-Up approach consists on the synthesis of graphene starting with carbon atoms or molecules and build up to graphene deposited over a substrate. On the other hand, in the Top Down approach, a pattern generated on a large scale (graphite) is reduced to graphene [6]. Graphite is the most known raw material used in the Top Down approach to synthesize reduced graphene oxide or powder graphene. Graphite oxide is obtained by treating graphite with strong oxidizing agents [7]. This material can be defined as a set of functionalized sheets of graphene formed by different oxygen functional groups, such as epoxides, hydroxides and carboxyl. The incorporation of oxygen groups into graphite makes its structure more hydrophobic, making possible the separation of its layers in aqueous solution by sonication [8,9] to obtain graphene oxide. In literature, several methods have been reported how synthesize graphite oxide such as Brodie [10], Staudenmaier [11] and Hummers Method [7] and its variations (Modified and Improved Hummers method) [12]. This material is considered an intermediate for the manufacture of reduced graphene oxide, which can be defined as a homogeneous material with structural defects, resulting from the elimination of a large portion of oxygen functional groups from the graphene oxide structure [13]. In general, reduced graphene oxide structure is similar to that of graphite oxide but it is not completely homogenous like graphene due to the occurrence of remaining functional groups [14]. Reduced graphene oxide can be obtained by removing the oxygen functional groups from graphite oxide following different strategies [15]: thermal reduction [16,17], photo reduction [18], electrochemical reduction [19], microwave reduction [20], solvothermal reduction [21], chemical reduction [5,22,23] by using a wide variety of reducing agents (hydroiodic acid, ascorbic acid, hydrazine, $NaBH_4$ or some metal hydrides [15]) and multiphase reduction [24–26]. Fig. 1 summarizes the advantages and disadvantages of the most important reduction techniques listed above.

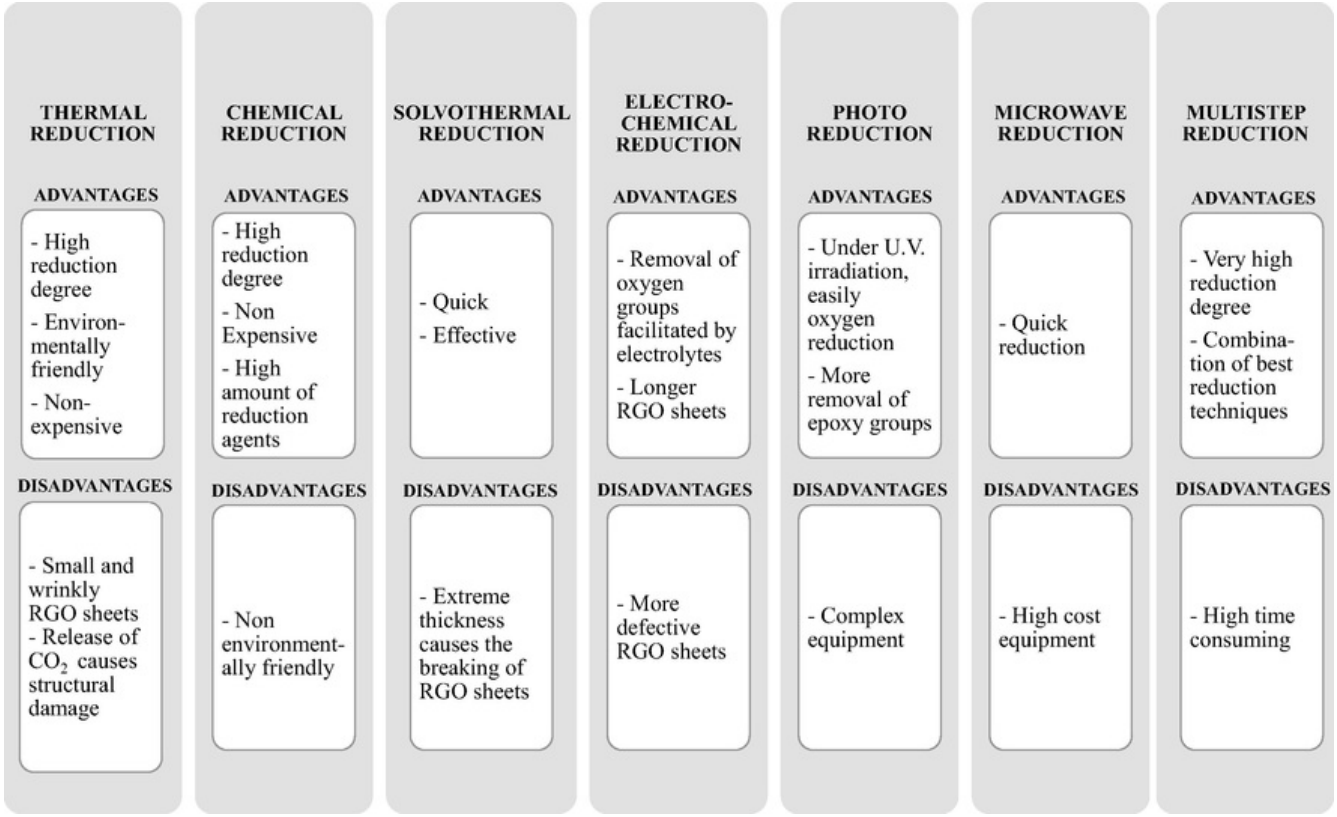

Fig. 1 Advantages and disadvantages of reduction strategies used in the production of reduced graphene oxide.

In this work, the structure and chemistry of different reduced graphene oxide samples prepared through different graphene–reduction strategies such as chemical, thermal and multiphase techniques, were compared. Graphene oxide can be reduced by using several reducing agents. In this work, hydrazine and ascorbic acid have been selected as the reducing agents. Hydrazine (N_2H_4) is a colourless flammable liquid with an ammonia-like odor, highly toxic and dangerously unstable unless handled in a solution [27] but it is a powerful and a convenient reductant because the by-products yielded in the reduction process are typically nitrogen gas and water. On the other hand, ascorbic acid or vitamin C, is a natural organic compound with antioxidant properties that owns both innocuous nature and environmentally friendly characteristics. It is a white solid that dissolves well in water to give mildly acidic solutions [28]. Ascorbic acid has been proposed recently as a potential agent to be used for graphene oxide reduction [29,30]. Chemical reduction technique involves the use of a liquid media, which can difficult the industrial production of reduced graphene oxide. However, other reduction procedures do not require this liquid media such as thermal reduction of graphene oxide. Even though, this procedure presents the disadvantage of the occurrence of a violent expansion of the material, which could damage the structure of the resulting material. A combination of both chemical and thermal reduction techniques was performed. The resulting products were compared to those separately obtained with each of the above-mentioned techniques.

2 Materials and methods

2.1 Materials

Graphite powder (<20 μm) was supplied by SIGMA-ALDRICH (Spain). Potassium permanganate ($KMnO_4$), sulfuric acid (H_2SO_4), chlorhydric acid (HCl), hydrogen peroxide (H_2O_2) and ethanol (CH_3CH_2OH) with a purity grade of 99%, 96%, 37%, 99.5% and 99.5%, respectively, were supplied by PANREAC (Spain). Monohydrate hydrazine with a purity grade of 98% was supplied by SIGMA-ALDRICH (Spain) and ascorbic acid with a purity grade of 99% was supplied by VWR (Spain).

2.2 Methods

2.2.1 Synthesis of graphite oxide (GrO)

Graphite oxide was synthesized following the Improved Hummers Method with slightly modifications [7]. A mixture of 15 g of graphite and 45 g of $KMnO_4$ (oxidizer agent) was slowly added to 400 mL of H_2SO_4 under constant agitation. The mixture was maintained at 50 °C for 3 h. Then, the mixture was added to a beaker containing a mixture of 400 g of flake ice and 3 mL of H_2O_2 to stop the oxidation reaction. The mixture was filtered under vacuum; then, it was washed with 200 mL of deionized water, HCl and CH_3CH_2OH. Finally, the compact cake was dried at 100 °C overnight.

2.2.2 Synthesis of graphene oxide (GO)

Graphene oxide synthesis was carried out by graphite oxide exfoliation. Thus, a mixture of 800 mg of graphite oxide and 800 mL of deionized water was introduced in a cooling jacketed reactor to maintain the solution at room temperature. The mixture was sonicated (50% amplitude and a complete cycle) for 2 h in order to separate the graphene sheets of graphite oxide to obtain graphene oxide [31]. The final mixture was centrifuged and the obtained solid was dried overnight at 80 °C.

2.2.3 Synthesis of reduced graphene oxide: reduction strategies

2.2.3.1 Chemical reduction Chemical reduction of graphene oxide was carried out using two different oxidizing agents: hydrazine and ascorbic acid. As commented above, hydrazine was selected because of its powerful reduction capacity but it is a very toxic product, which is also detrimental for the environment. For this reason, an alternative reducer agent, ascorbic acid, was proposed. This agent is innocuous and environmentally friendly.

The chemical reduction with hydrazine was carried out by mixing 800 mg of graphene oxide solution with 800 mg of hydrazine monohydrate. The mixture was maintained under constant agitation at 90 °C for 3 h [23]. After reduction, the dissolution was centrifuged and the product (**H**ydrazine **R**educed **G**raphene **O**xide (H-RGO)) was filtered and washed until pH = 7 with deionized water to eliminate the remaining hydrazine. Finally, the obtained solid was dried at 80 °C overnight.

The chemical reduction with ascorbic acid was carried out by mixing 800 mg of graphene oxide solution and 800 mg of ascorbic acid. The reduction was maintained under constant agitation for 48 h at room temperature [29]. After the reduction, the dissolution was centrifuged and the obtained product (**A**scorbic acid **R**educed **G**raphene **O**xide (A-RGO)) was filtered and washed several times with deionized water (until pH = 7) to remove the remaining acid. Finally, the obtained solid was dried overnight at 80 °C.

2.2.3.2 Thermal reduction Thermal reduction process was carried out by introducing 5 g of graphite oxide in a laboratory drying oven at low temperatures (250 °C). The carbon material expansion took place after a certain time (always in the range 20–40 min), separating the graphene layers and, removing some oxygen functional groups from the structure. The obtained product was named as **T**hermally **R**educed **Gr**aphite **O**xide (T-RGrO).

After thermal reduction, 800 mg T-RGrO was sonicated (30% amplitude) for 2 h in 800 mL of deionized water to complete its exfoliation obtaining **T**hermally **R**educed **G**raphene **O**xide (T-RGO).

2.2.3.3 Multiphase reduction Multiphase reduction was carried out by combining the previously commented reduction strategies (thermal reduction followed by the chemical one, using both hydrazine and ascorbic acid as reducing agents). The product obtained by thermal reduction followed by hydrazine chemical reduction was named as **H**ydrazine **M**ulti**P**hase **R**educed **G**raphene **O**xide (HMP-RGO) whereas the product obtained by thermal reduction followed by ascorbic acid chemical reduction was named as **A**scorbic acid **M**ulti**P**hase **R**educed **G**raphene **O**xide (AMP-RGO).

2.3 Characterization techniques

The Fourier transform infrared (FTIR) spectra analysis was carried out on a SPECTRUM TWO spectrometer (Perkin Elmer, Inc) with a scan resolution of 0.5 cm^{-1}. Raman spectrums were obtained with a SENTERRA spectrometer with a grating of 600 lines per mm and a laser wavelength of 532 nm at a very low laser power level (<1 mW), to avoid any heating effect. Thermogravimetric analysis (TGA) data were recorded on a METTLER TOLEDO TGA/DSC1 instrument. Samples were heated from 30 to 1000 °C at 10 °C/min under a reactive atmosphere of 21% of oxygen and 79% of nitrogen. The morphology of the samples was observed with Scanning Electron Microscopy (SEM) (Phenom ProX) with a field emission gun with a resolution of 15 kV and a magnification of 2000×. Elemental analysis was carried out using the EDX software of SEM equipment. The powder X-ray diffraction (XRD) analysis was performed on a diffractometer (PHILIPS, PW-1711) with CuKα radiation (λ = 1.5404 Å). The samples were scanned at a rate of 0.02° $step^{-1}$ over the range 5° ≤ 2θ ≤ 90° (scan time = 2 s $step^{-1}$) and the diffractograms were compared with the PDF-ICDD references. Characteristic crystallographic parameters (interlaminar space (d_{002}); crystal stack height (L_c); in-plane crystallite size (L_a) and number of graphene layers in the crystal (N_c)) were determined as follows [32,33]:

$$d_{002} = \frac{\lambda}{2 \cdot \mathrm{sen}\theta_1}; \quad L_c = \frac{k_1 \cdot \lambda}{FWHM \cdot \cos\theta_1};$$

$$La(nm) = \frac{k_2 \cdot \lambda}{FWHM \cdot \cos\theta_2}; \quad N_c = \frac{L_c}{d_{002}}$$

where:

- λ, radiation wavelength (λ = 0.15404 nm)
- θ_1, [0 0 2] and [0 0 1] diffraction peak position (°)
- θ_2, [1 0 0] diffraction peak position (°)
- k_1, form factor (k = 0.9)
- k_2, Warren Form Factor constant (k = 1.84)
- FWHM, width at half height of the corresponding diffraction peak (rad)

3 Results and discussion

Different reduction methods (e.g. chemical, thermal and multiphase techniques) have been used to maximize the removing of oxygen functional groups in graphite oxide.

Fig. 2 shows the oxygen and carbon atoms content (wt.%) of the different graphene-based materials prepared in this study. Graphite, the non-oxidized raw material, is composed by 100% of carbon atoms. After the oxidation process to obtain graphite oxide (GrO), the content of oxygen as part of a functional group was increased to up 51.7%. Graphene oxide (GO), obtained after GrO exfoliation by means of sonication, showed an oxygen content like that of GrO (52%) which seems logical due to sonication is a physical process and not a chemical one.

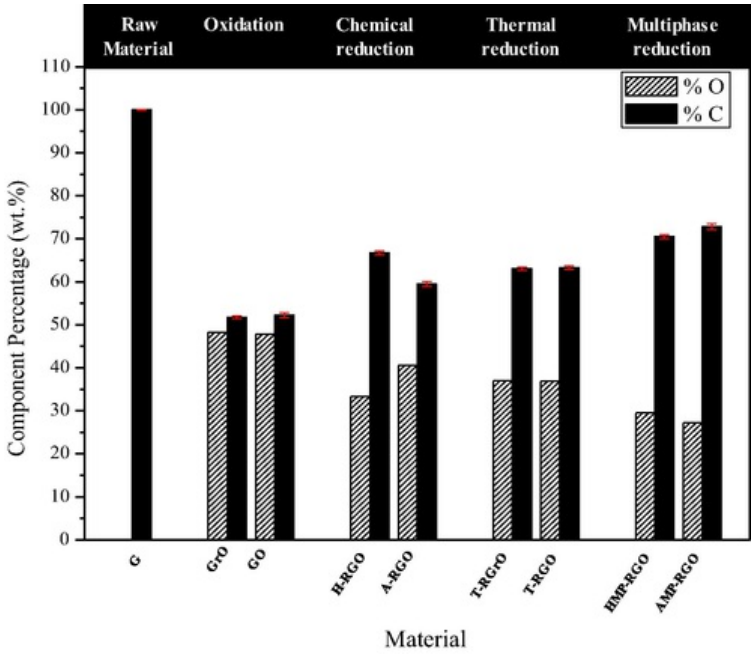

Fig. 2 Elemental analysis (C and O content) of graphite (G), graphite oxide (GrO), graphene oxide (GO) and reduced graphene oxide samples.

It was confirmed that hydrazine was more effective than ascorbic acid as reducing agent, because oxygen functional groups were reduced from 52% (graphene oxide) to 33.3% in H-RGO and 40.5% in A-RGO, respectively. Thus, only 22% of the oxygen groups were removed using ascorbic acid whereas about 36% of them were removed using hydrazine.

Removal of oxygenated functional groups by thermal reduction is mainly due to CO and CO_2 evolution, which involves the generation of atomic vacancies and voids into the structure. Although the elimination of an isolated functional group in graphene (e.g., an epoxy group removed as CO) is energy costly, the process is enhanced both thermodynamic and kinetically in presence of more oxygen functional groups located ones next to other. In other words, the oxygen functional group energy stabilizes both the final structure and the transition states [34]. The high oxygen density in graphite oxide allows to eliminate much of the oxygen present therein at unusually low temperatures (150–300 °C). The remaining oxygen functional groups in the structure are most likely in the form of isolated groups, thus requiring much higher temperatures for their removal. Recent studies have shown that elevated temperatures (1050 °C) are necessary to completely remove oxygen groups of graphene oxide [34]. Finally, temperatures higher than 2000 °C allows to remove structural defects remaining in this material.

After the thermal reduction process, the percentage of oxygen was decreased from 51.7% (GrO) to 37% (T-RGrO), removing around 28% of oxygen functional groups. Again, the T-RGrO exfoliation by sonication to obtain T-RGO did not affect the oxygen percentage, which is kept practically constant (37%).

Finally, elemental analysis of the reduced graphene samples prepared by the multiphase method (HMP-RGO and AMP-RGO, when hydrazine and ascorbic acid were used as the reducing agents, respectively) demonstrated the effectiveness of this oxygen removing technique. Thus, around 30% and 27% of the carbon atoms remained in the HMP-RGO and AMP-RGO structures, respectively, after the reduction process. Thermal reduction manages to remove the most labile oxygen groups, many of which are attacked with great efficacy using a single step of chemical reduction with hydrazine due to the great reducing power of this chemical compound. Therefore, when hydrazine is used in the multiphase method, these oxygenated groups have already been eliminated, so that the great reductive power of hydrazine is wasted. However, everything seems to indicate according to the achieved results that, during the multiphase reduction using ascorbic acid, were attacked oxygen functional groups which, although weakened by the previous thermal reduction, were not totally eliminated.

Consequently, AMP-RGO is the material in which higher degree of reduction was attained.

Results obtained by elemental analysis was corroborated by results reported in bibliography [35]. The amount of oxygen functional groups remove from graphite oxide is bigger for multiphase reduction method, followed by chemical reduction with hydrazine, thermal reduction and finally, RGO reduced using ascorbic acid as reducing agent is the one which presented more oxygen functional groups in its structure.

Fig. 3 shows the TGA and DTG profiles corresponding to graphite (G), graphite oxide (GrO) and graphene oxide (GO). Regarding graphite, the corresponding TGA curve confirmed its high thermal stability, which did not start its decomposition until 650 °C, losing around 92% of its mass at 900 °C [36]. Graphite oxide and graphene oxide showed similar TGA curves. In both cases, three different weight loss steps could be differentiated. The first one (I), appearing between 0 and 200 °C, was mainly due to the elimination of both water solvent molecules and the decomposition of the more labile oxygen functional groups [37]. Regarding GO, the weight loss corresponding in this first step (21%) was lower than that observed for GrO (37%), indicating that sonication and subsequent drying of graphite oxide considerably reduced the amount of water molecules in the resulted material. The second weight loss step (II), occurring between 200 and 475 °C, was due to the removal of the more stable oxygen groups. Similar weight loss was observed for both GrO and GO (27% and 28%, respectively), indicating that both materials had the same stable oxygen functional groups. Finally, a third step (III) for temperatures above 475 °C was observed, which was a consequence of the material thermal degradation (unstable carbon remaining in the structure yields CO and CO_2 [38]), losing around 30% of the remaining mass.

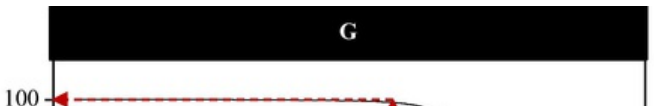

ELSEVIER_APT_1739

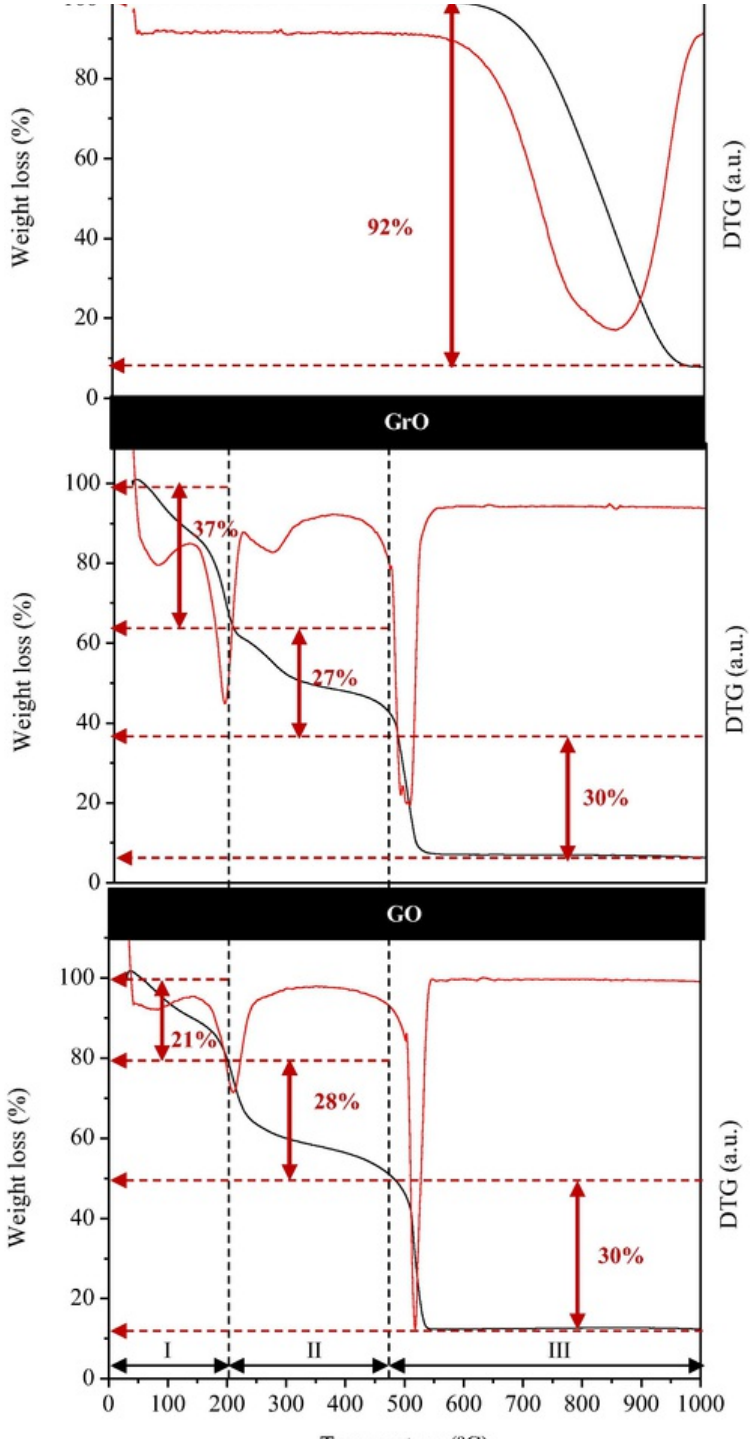

Temperature (°C)

Fig. 3 TGA and DTG curves of graphite (G), graphite oxide (GrO) and graphene oxide (GO).

Thermogravimetric analyses results were corroborated by FTIR (Fig. 4). FTIR spectrum of graphite showed the absence of bonds different from those expected in its structure. After the oxidation process, several functional groups were incorporated into the structure (Table 1) [38,39].

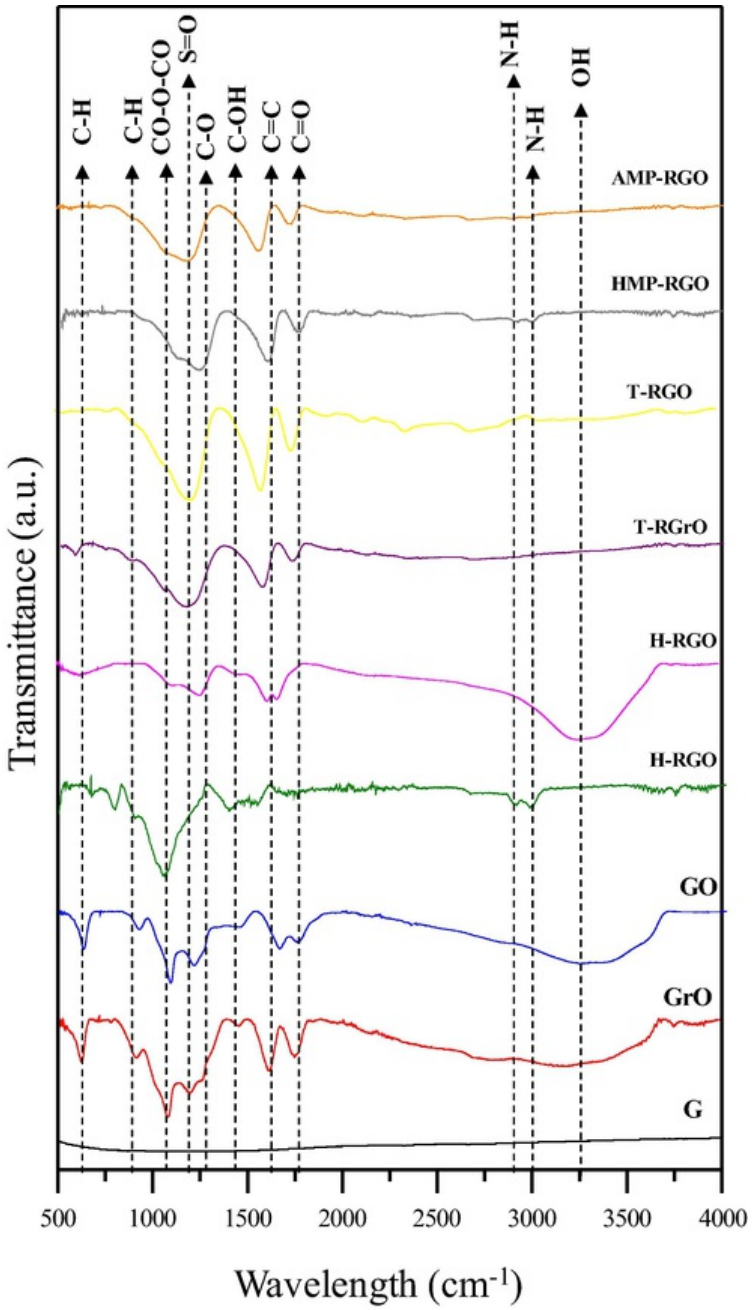

Fig. 4 FTIR analyses of graphite (G), graphite oxide (GrO), graphene oxide (GO) and reduced graphene oxide samples.

Table 1 Functional groups present in graphite (G), graphite oxide (GrO), graphene oxide (GO) and reduced graphene oxide samples [40].

Functional groups	Wavelength (cm^{-1})
C—H (CH group)	755–900
CO—O—CO (Anhydride group)	1050
C—O (Ether group)	1275
C=C (Alkene group)	1650
C=O (Ester, aldehyde and carboxylic acid groups)	1720–1780
N—H (Amine group)	2800–3000
C—OH (Hydroxyl group)	1420, 3700

Fig. 5 shows TGA and DTG curves corresponding to the reduced graphene oxide samples obtained through different reduction strategies. Three different weight loss steps were also observed, confirming the superior reduction power of hydrazine if is compared to that of the ascorbic acid. Thus, H-RGO sample showed a minimum weight loss in step (I) (≈2%), which was linked to the elimination of the most labile oxygen groups after the reduction process. Nevertheless, sample A-RGO showed a step (I) weight loss of 25%, demonstrating that the more labile oxygen groups were not completely removed from graphene oxide structure after the reduction process. On the other hand, the weight loss corresponding to step (II) was quite similar for both chemically reduced samples, being the weight loss associated to step (III) higher in sample H-RGO (66%) than in A-RGO (45%) due to its higher amount of unstable carbon (see elemental analysis results). These results were also corroborated by FTIR analysis (Fig. 4). Thus, in sample H-RGO the broad band corresponding to hydroxyl groups (around 3700 cm^{-1}) disappeared due to hydrazine attacks to the OH groups by nucleophilic substitution [41] causing different hydrogen bond rearrangements [38]. On the other hand, two new small bands at 2899 cm^{-1} and 3000 cm^{-1} were appreciated due to the tendency of the oxygen functional groups to form complex structures with nitrogen (azide complex). These results are in good agreement with those reported by Chua et al. [42], who has demonstrated through a computational study that hydrazine reduction removed favourably OH groups present in the graphene oxide basal plane.

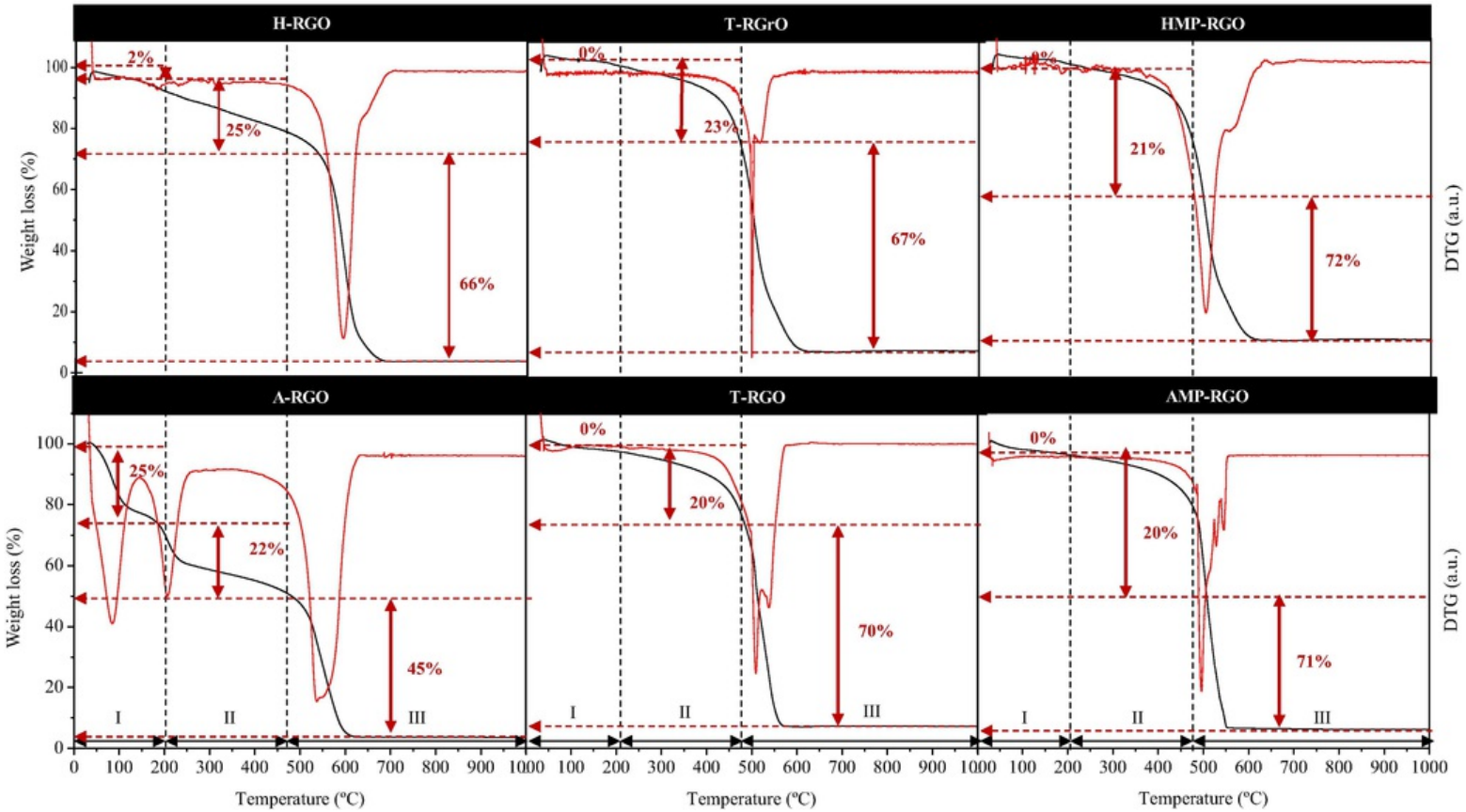

Fig. 5 TGA and DTG curves of reduced graphene oxide samples.

For its part, A-RGO spectrum showed that the hydroxyl groups were not completely removed after the reduction process. Other oxygen functional groups that were partially removed after hydrazine/ascorbic acid reduction were C═O groups (1770 cm^{-1}) associated to esters, aldehydes and carboxylic acids, and C═C groups (1650 cm^{-1}), corresponding to phenolic rings, which is a consequence of their interaction with the reducing agent causing bond deformations [38].

TGA curves corresponding to thermally reduced samples (T-RGrO and T-RGO) did not shown any weight loss during step (I) confirming the elimination of almost all the labile functional groups and water molecules. Weight loss corresponding to step (II) was quite similar in samples T-RGrO and T-RGO (around 20–23%), indicating that most of the more stable oxygen groups remained in the structure after thermal reduction. Finally, material thermal degradation started at temperatures above 500–550 °C, showing a step (III) weight loss of around 70% [17].

FTIR analysis of samples T-RGrO and T-RGO showed that hydroxyl groups were practically removed after the thermal reduction, disappearing completely the broadband occurring at around 3700 cm^{-1} [38,39]. Furthermore, bands corresponding to C—O (1275 cm^{-1}) and C═O groups (1770 cm^{-1}) were partially removed after the violent thermal expansion happened.

TGA curves corresponding to multiphase reduced samples (HMP-RGO and AMP-RGO) were similar to those of the thermally reduced ones; e.g. TGA curves did not show any weight loss in step (I) confirming the elimination of almost all the labile functional groups and water molecules. Around 20% of the mass was lost in step (II) due to the partial removal of the more stable oxygen groups. Finally, total thermal decomposition of the reduced graphene oxide samples took place around 550 °C. Again, these results were confirmed by FTIR analyses, where no band associated to —OH groups was observed. In addition, C—O or C═O groups were also partially removed after multiphase reduction. Bands associated to complexes structures with nitrogen (complex azide) appeared in sample HMP-RGO due to the action of the hydrazine [42]. Regardless of the reduction technique, C—H groups (755–900 cm^{-1}) were almost completely removed.

Raman spectroscopy is considered a very interesting tool in the study of carbon nanomaterials due to its quickness and trustworthiness [43]. Raman spectrum and the most characteristics Raman parameters corresponding to both GrO and GO samples are shown in Fig. 6 and Table 2, respectively. The two characteristic peaks (D and G) could be easily differentiated. D peak, which appears around 1348 cm^{-1}, indicates the presence of imperfections in the graphitic structure of carbon atoms at the layer edges [44]. G peak is related to the movement of pairs of carbon atoms linked by sp^2 bonds and this is located at 1586 cm^{-1}. This peak is commonly related to the graphitic order [45]. Thus, the broad G band and the more prominent D one associated with GrO and GO (when compared to graphite) indicate a reduction in the size of the sp^2 domains due to oxidation. The relationship between the intensities of the two peaks (I_D/I_G) will be used to compare the way in which the structural disorder grows in the graphitic network. The locations of both D and G bands and the ratio between their intensities are consistent with the characteristic values reported elsewhere [41].

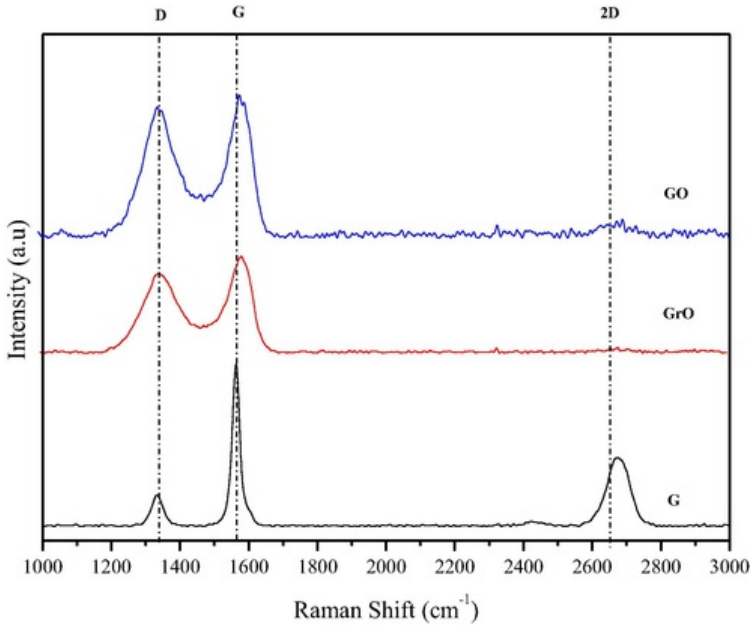

Fig. 6 Raman spectra of graphite (G), graphite oxide (GrO) and graphene oxide (GO).

Table 2 Raman and XRD characteristic parameters of graphite (G), graphite oxide (GrO) and graphene oxide (GO) and reduced graphene oxide samples.

	XRD						RAMAN	
Sample	2θ (°) $_{[0\,0\,2]\text{ or }[0\,0\,1]_{peak}}$	L_c (nm)	d_{002} (nm)	N_c	2θ (°) $_{[1\,0\,0]_{peak}}$	L_a (nm)	I_D/I_G	L_D (nm)
G	26.58	37.10	0.34	111	–	–	0.19	23.2
GrO	9.96	4.43	0.89	5	42.43	11.03	0.94	10.4
GO	9.15	3.75	0.97	4	42.77	5.79	0.99	10.2
H-RGO	24.19	1.06	0.37	3	43.11	2.63	1.25	9
A-RGO	23.56	1.38	0.38	4	43.51	4.55	1.16	9.4
T-RGrO	23.7	1.61	0.37	4	43.33	4.50	0.96	10.3
T-RGO	23.02	0.92	0.39	3	43.68	3.59	0.97	10.3
HMP-RGO	21.4	0.96	0.40	2	43.57	5.17	1.18	9.3
AMP-RGO	22.09	0.97	0.41	2	43.24	6.28	1.15	9.4

When pristine graphite was oxidized to GrO, the I_D/I_G ratio of the resulting material significantly increased indicating a higher level of structural disorder and a larger number of defects in the graphene layers due to the oxidation process. After sonication to obtain GO, I_D/I_G relationship in the resulting material lightly increased, indicating that exfoliation process also incorporated further defects in the structure. Logically, the distance between defects (determined as $LD = \sqrt{C(\lambda)/(ID/IG)}$, being $C(\lambda) = 102\,nm^2$ [46], decreased from graphite to both GrO and GO [39].

Results derived from Raman spectra were corroborated by XRD analysis. Fig. 7 shows X-ray diffraction patterns whereas Table 2 lists the characteristic XRD parameters corresponding to G, GrO and GO. Graphite showed a [0 0 2] peak at a 2θ value of around 26.6°, which is consistent with a separation between layers (d_{002}) of 0.34 nm. After oxidation, [0 0 2] peak disappeared, appearing two new peaks: [0 0 1] at $2\theta \approx 9.9°$ and [1 0 0] at $2\theta \approx 42.5°$. As consequence, the interlayer distance (d_{002}) clearly increased while the crystal domains (both the crystal stack height, L_c and the in-plane crystallite size, L_a) decreased after the oxidation process. The d_{002} increase was attributed to the expansion caused by the presence of oxygen functional groups and water molecules located in the interlayer galleries of the hydrophilic GrO and GO samples. For its part, crystallite domains reduction indicated that an increase in the structural disorder occurred after the oxidation process (GrO)

and subsequent exfoliation to yield GO. Finally, the number of layers in the stacking structure (N_c) decreased markedly after graphite oxidation and subsequent sonication, which was related not only to the graphene layer separation but also to the crystallinity loss in the ultimate material.

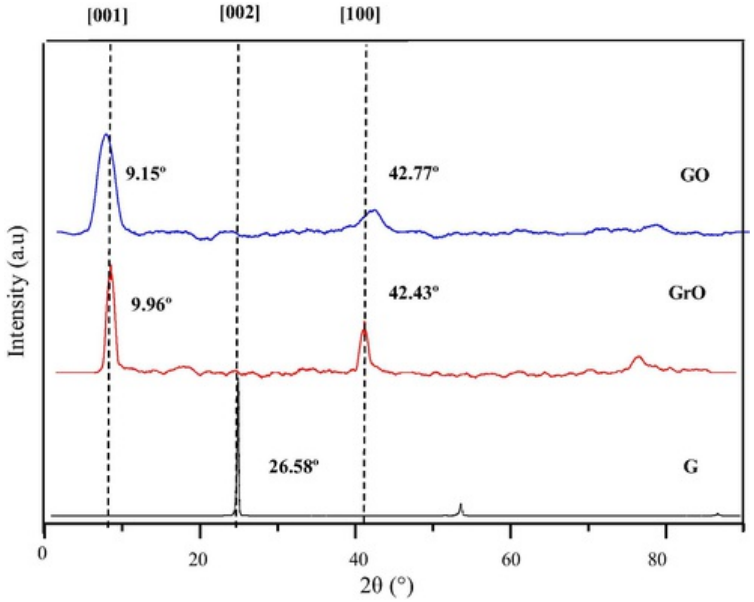

Fig. 7 XRD spectra of graphite (G), graphite oxide (GrO) and graphene oxide (GO).

Raman spectra and characteristics Raman parameters corresponding to the reduced graphene samples are shown in Fig. 8 and Table 2, respectively. As observed, I_D/I_G ratio increased after chemical reduction indicating that not only the oxidation but also the chemical reduction process contributed to an increase of the structural disorder, which was much higher in sample H-RGO than in sample A-RGO. As above mentioned, hydrazine removed oxygen functional groups more efficiently than ascorbic acid, as corroborated by elemental and FTIR analyses.

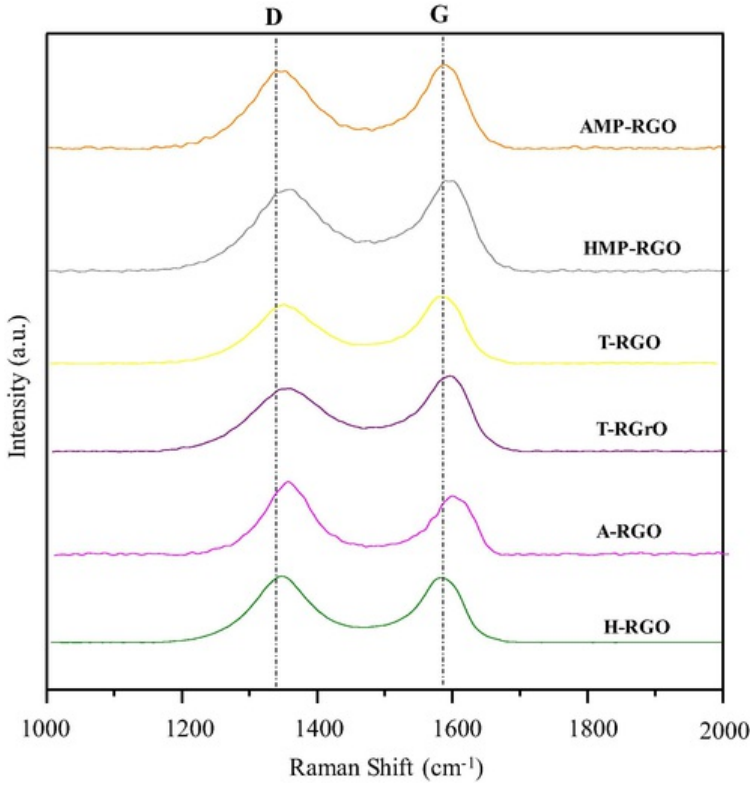

Fig. 8 Raman spectra of reduced graphene oxide samples.

Both chemically reduced products showed characteristics values of I_D/I_G, which ranged from 1.14 to 1.28 [39]. As expected, distance between defects (L_D) was higher for sample A-RGO due to it presented a lower number of defects.

XRD analysis (Fig. 9) showed that when GO was chemically reduced peak [0 0 1] was widener and shifted to higher 2θ values, due to the tendency of the reduced material to recover the original graphite structure although the crystallinity of the resulting material is reduced. As observed, d_{002} and crystal domains (Lc and La) decreased after chemical reduction due to the structural disorder increase, obtaining a higher reduction in the case of sample H-RGO due to the above mentioned high reduction power of hydrazine.

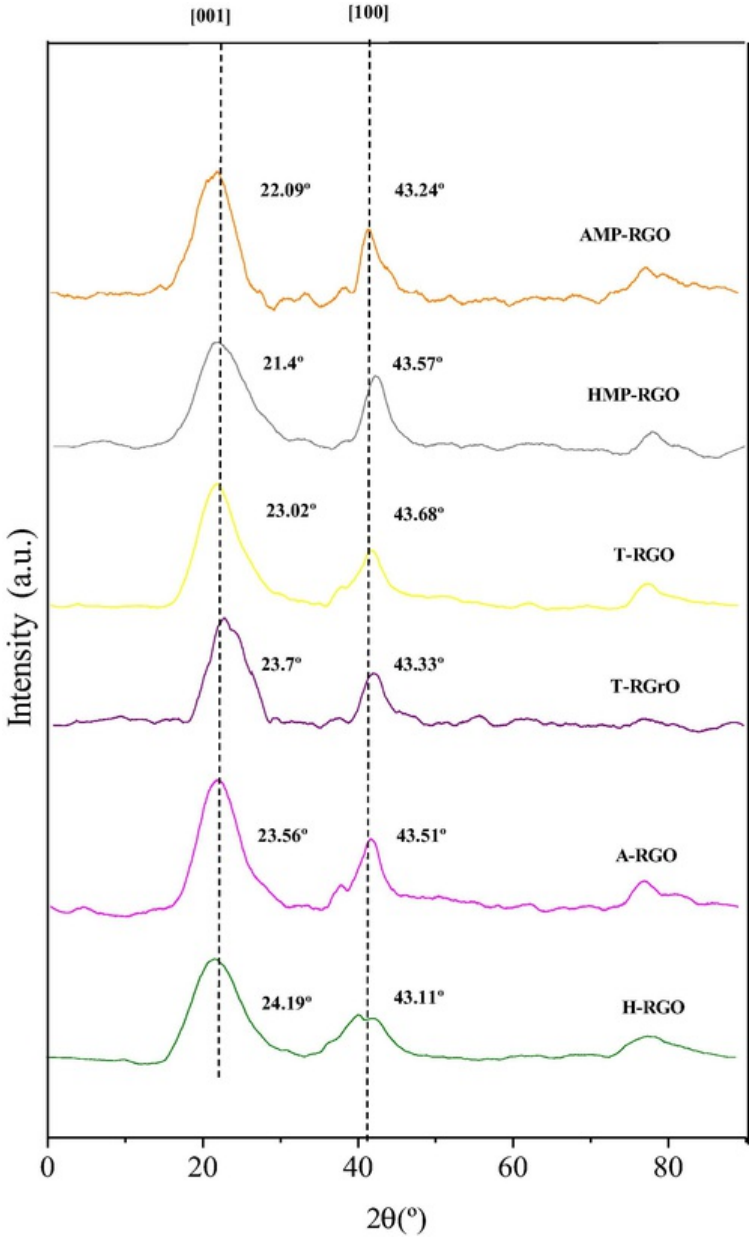

Fig. 9 XRD spectra of reduced graphene oxide samples.

On the other hand, after thermal reduction both I_D/I_G ratio and distance between defects (L_D) presented a similar tendency as the non-reduced material (GrO). In other words, thermal expansion, which removed mainly the more labile oxygen functional groups (mostly located out of the basal plane [5]), did not practically contributed to add further structural defects in the resulting reduced material. Similar Raman results were obtained for samples T-RGrO and T-RGO, which agree well with thermal and elemental analysis results.

XRD patterns of samples T-RGrO and T-RGO were quite similar. Again, d_{002} and crystal domains decreased after the reduction process. Note that L_a and L_c values considerably decreased after the exfoliation indicating that the T-RGrO sonication to obtain T-RGO caused not only the exfoliation of the structure but also the breakage of the crystal structure.

Finally, Raman spectra of multiphase reduced samples showed that when hydrazine was used as the reducing agent the number of defects in the final material (HMP-RGO) were slightly higher than that evaluated when ascorbic acid was used (AMP-RGO), due to hydrazine attacks more intensely the structure, increasing the number of defects. This fact was also evidenced by XRD measurements where crystal domains were slightly higher in sample AMP-RGO than in sample HMP-RGO.

Fig. 10 shows the morphological properties of the different materials studied evaluated by Scanning Electron Microscopy (SEM). Graphite structure showed a crystalline platelet-like structure with well-defined sheets. After the oxidation process, GrO sample presented a damaged structure. GO showed a single flakes structure with relatively large surface, resembling a thin curtain, which indicates that a very good exfoliation took place after the oxidation process [38]. SEM images corresponding to reduced samples showed structures with a more developed surface, resembling cluttered products with poor crystallinity, as demonstrated by the XRD analysis.

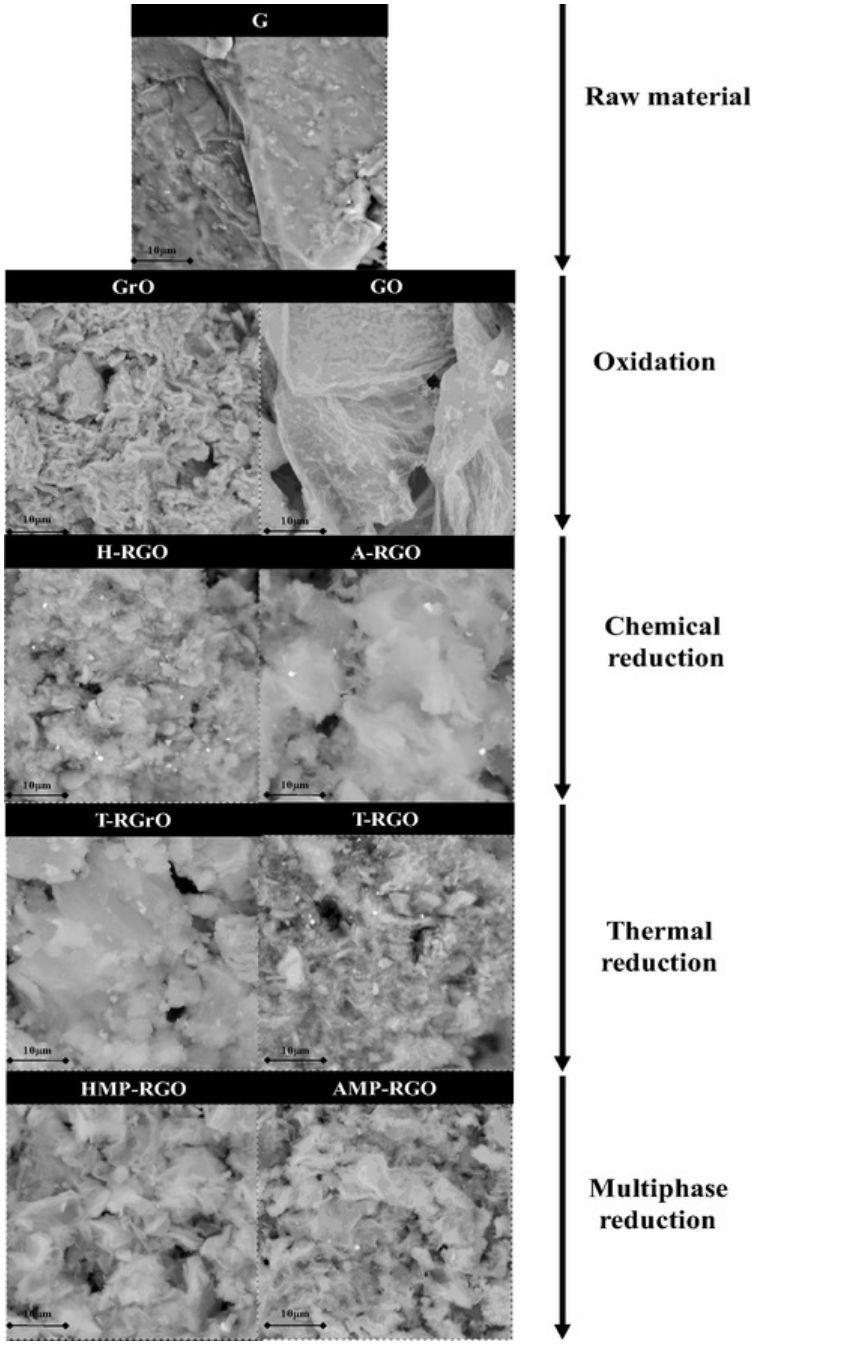

Fig. 10 SEM images of graphite (G), graphite oxide (GrO), graphene oxide (GO) and reduced graphene oxide samples.

4 Conclusions

In this manuscript, different graphene reduction strategies to synthesize reduced graphene oxide were reported. An optimization of the most knowledge oxidation route reported in the literature (Improved Hummers Method) was used to obtain graphite oxide. Subsequently, different sets of reduced graphene oxide powders were synthesized using three different reduction routes: chemical reduction, using hydrazine and ascorbic acid as reduction agents, thermal reduction and multiphase reduction. A total of eight separate final products were characterized to obtain the most effective reduction strategy.

Obtained results showed that, multiphase reduction method, resulting from the combination of more than one reduction route, specifically thermal and chemical ones, led to an effective removal of oxygen functional groups. Thus, a mild thermal treatment followed by a chemical reduction using ascorbic acid as the reducing agent, showed a functional groups reduction of 47%. A detailed characterization of the resulting materials confirmed the removal of the most labile oxygen functional groups and some of the more stable ones, without appreciating an increase in the number of structural defects and limiting the extension of lattice reconstruction after reduction. In this manuscript, it has been clearly demonstrated that, the reduced graphene oxide structure is highly dependent on the reduction strategy and, because of the promising results achieved, it would be convenient in the near future not only to optimize the developed multiphase reduction method in order to increase productivity, but also to apply this method using other reducing agents that are low cost and that respectful with the environment.

Acknowledgements

The present work was performed within the frame of the NANOLEAP project. This project has received funding from the European Union's Horizon 2020 research and innovation programme under grant agreement No. 646397.

References

[1]
Q. Su, S. Pang, V. Alijani, C. Li, X. Feng and K. Müllen, Composites of graphene with large aromatic molecules, *Adv. Mater.* **21**, 2009, 3191–3195.

[2]
Y. Zhu, S. Murali, W. Cai, X. Li, J.W. Suk, J.R. Potts and R.S. Ruoff, Graphene and graphene oxide: synthesis, properties, and applications, *Adv. Mater.* **22**, 2010, 3906–3924.

[3]
W. Choi, I. Lahiri, R. Seelaboyina and Y.S. Kang, Synthesis of graphene and its applications: a review, *Crit. Rev. Solid State Mater. Sci.* **35**, 2010, 52–71.

[4]
S.J. Chae, F. Güneş, K.K. Kim, E.S. Kim, G.H. Han, S.M. Kim, H.-J. Shin, S.-M. Yoon, J.-Y. Choi, M.H. Park, C.W. Yang, D. Pribat and Y.H. Lee, Synthesis of large-area graphene layers on poly-nickel substrate by chemical vapor deposition: wrinkle formation, *Adv. Mater.* **21**, 2009, 2328–2333.

[5]
C.K. Chua and M. Pumera, Chemical reduction of graphene oxide: a synthetic chemistry viewpoint, *Chem. Soc. Rev.* **43**, 2014, 291–312.

[6]
J.M. Tour, Top-down versus bottom-up fabrication of graphene-based electronics, *Chem. Mater.* **26**, 2014, 163–171.

[7]
W.S. Hummers, Jr and R.E. Offeman, Preparation of graphitic oxide, *J. Am. Chem. Soc.* **80**, 1958, 1339.

[8]
S. Park and R.S. Ruoff, Chemical methods for the production of graphenes, *Nat Nano* **4**, 2009, 217–224.

[9]
G. Shao, Y. Lu, F. Wu, C. Yang, F. Zeng and Q. Wu, Graphene oxide: the mechanisms of oxidation and exfoliation, *J. Mater. Sci.* **47**, 2012, 4400–4409.

[10]
L.L. Abel, B.B. Levy, B.B. Brodie and F.E. Kendall, A simplified method for the estimation of total cholesterol in serum and demonstration of its specificity, *J. Biol. Chem.* **195**, 1952, 357–366.

[11]
L. Staudenmaier, Verfahren zur darstellung der graphitsäure, *Berichte der Deutschen Chemischen Gesellschaft* **31**, 1898, 1481–1487.

[12]
D.C. Marcano, D.V. Kosynkin, J.M. Berlin, A. Sinitskii, Z. Sun, A. Slesarev, L.B. Alemany, W. Lu and J.M. Tour, Improved synthesis of graphene oxide, *ACS Nano* **4**, 2010, 4806–4814.

[13]
K. Erickson, R. Erni, Z. Lee, N. Alem, W. Gannett and A. Zettl, Determination of the local chemical structure of graphene oxide and reduced graphene oxide, *Adv. Mater.* **22**, 2010, 4467–4472.

[14]
A. Bagri, C. Mattevi, M. Acik, Y.J. Chabal, M. Chhowalla and V.B. Shenoy, Structural evolution during the reduction of chemically derived graphene oxide, *Nat. Chem.* **2**, 2010, 581–587.

[15]
S. Pei and H.M. Cheng, The reduction of graphene oxide, *Carbon* **50**, 2012, 3210–3228.

[16]
S.H. Huh, Thermal Reduction of Graphene Oxide, Physics and Applications of Graphene - Experiments, in: D.S. Mikhailov (Ed.), InTech, 2011.

[17]
M.J. McAllister, J.L. Li, D.H. Adamson, H.C. Schniepp, A.A. Abdala, J. Liu, M. Herrera-Alonso, D.L. Milius, R. Car, R.K. Prud'homme and I.A. Aksay, Single sheet functionalized graphene by oxidation and thermal expansion of graphite, *Chem. Mater.* **19**, 2007, 4396–4404.

[18]
Y. Zhang, L. Guo, S. Wei, Y. He, H. Xia, Q. Chen, H.B. Sun and F.S. Xiao, Direct imprinting of microcircuits on graphene oxides film by femtosecond laser reduction, *Nano Today* **5**, 2010, 15–20.

[19]
G.K. Ramesha and N.S. Sampath, Electrochemical reduction of oriented graphene oxide films: an in situ Raman spectroelectrochemical study, *J. Phys. Chem. C* **113**, 2009, 7985–7989.

[20]
Y. Zhu, S. Murali, M.D. Stoller, A. Velamakanni, R.D. Piner and R.S. Ruoff, Microwave assisted exfoliation and reduction of graphite oxide for ultracapacitors, *Carbon* **48**, 2010, 2118–2122.

[21]
H. Wang, J.T. Robinson, X. Li and H. Dai, Solvothermal reduction of chemically exfoliated graphene sheets, *J. Am. Chem. Soc.* **131**, 2009, 9910–9911.

[22]
S. Stankovich, D.A. Dikin, R.D. Piner, K.A. Kohlhaas, A. Kleinhammes, Y. Jia, Y. Wu, S.T. Nguyen and R.S. Ruoff, Synthesis of graphene-based nanosheets via chemical reduction of exfoliated graphite oxide, *Carbon* **45**, 2007, 1558–1565.

[23]
S. Park, J. An, J.R. Potts, A. Velamakanni, S. Murali and R.S. Ruoff, Hydrazine-reduction of graphite- and graphene oxide, *Carbon* **49**, 2011, 3019–3023.

[24]
W. Gao, L.B. Alemany, L. Ci and P.M. Ajayan, New insights into the structure and reduction of graphite oxide, *Nat. Chem.* **1**, 2009, 403–408.

[25]
Y. Si and E.T. Samulski, Synthesis of water soluble graphene, *Nano Lett.* **8**, 2008, 1679–1682.

[26]
C. Nethravathi and M. Rajamathi, Chemically modified graphene sheets produced by the solvothermal reduction of colloidal dispersions of graphite oxide, *Carbon* **46**, 2008, 1994–1998.

[27]
J.-P. Schirmann, P. Bourdauducq, Hydrazine, in: Ullmann's Encyclopedia of Industrial Chemistry, Wiley-VCH Verlag GmbH & Co. KGaA, 2000.

[28]
M.Y. Lachapelle and G. Drouin, Inactivation dates of the human and guinea pig vitamin C genes, *Genetica* **139**, 2010, 199–207.

[29]
J. Zhang, H. Yang, G. Shen, P. Cheng and S. Guo, Reduction of graphene oxide vial-ascorbic acid, *Chem. Commun.* **46**, 2010, 1112–1114.

[30]
H. Ding, S. Zhang, J.T. Chen, X.P. Hu, Z.F. Du, Y.X. Qiu and D.L. Zhao, Reduction of graphene oxide at room temperature with vitamin C for RGO-TiO_2 photoanodes in dye-sensitized solar cell, *Thin Solid Films* **584**, 2015, 29–36.

[31]
M. Choucair, P. Thordarson and J.A. Stride, Gram-scale production of graphene based on solvothermal synthesis and sonication, *Nat. Nanotechnol.* **4**, 2009, 30–33.

[32]
L. Stobinski, B. Lesiak, A. Malolepszy, M. Mazurkiewicz, B. Mierzwa, J. Zemek, P. Jiricek and I. Bieloshapka, Graphene oxide and reduced graphene oxide studied by the XRD, TEM and electron spectroscopy methods, *J. Electron Spectrosc. Related Phenomena* **195**, 2014, 145–154.

[33]
B.E. Warren, X-ray diffraction in random layer lattices, *Phys. Rev.* **59**, 1941, 693–698.

[34]
T. Sun, S. Fabris and S. Baroni, Surface precursors and reaction mechanisms for the thermal reduction of graphene basal surfaces oxidized by atomic oxygen, *J. Phys. Chem. C* **115**, 2011, 4730–4737.

[35]
A.A. Shamsabadi, A. Kargari, M.B. Babaheidari, S. Laki and H. Ajami, Role of critical concentration of PEI in NMP solutions on gas permeation characteristics of PEI gas separation membranes, *J. Ind. Eng. Chem.* **19**, 2013, 677–685.

[36]
D.M. Crumpton, R.A. Laitinen, J. Smieja and D.A. Cleary, Thermal analysis of carbon allotropes: an experiment for advanced undergraduates, *J. Chem. Educ.* **73**, 1996, 590–591.

[37]
M.J. Fernández-Merino, L. Guardia, J.I. Paredes, S. Villar-Rodil, P. Solís-Fernández, A. Martínez-Alonso and J.M.D. Tascón, Vitamin C is an ideal substitute for hydrazine in the reduction of graphene oxide suspensions, *J. Phys. Chem. C* **114**, 2010, 6426–6432.

[38]
V. Loryuenyong, K. Totepvimarn, P. Eimburanapravat, W. Boonchompoo and A. Buasri, Preparation and characterization of reduced graphene oxide sheets via water-based exfoliation and reduction methods, *Adv. Mater. Sci. Eng.* **2013**, 2013, 5.

[39]
S. Eigler, C. Dotzer and A. Hirsch, Visualization of defect densities in reduced graphene oxide, *Carbon* **50**, 2012, 3666–3673.

[40]
Chemistry, Infrared Spectroscopy Absorption Table, 2014.

[41]
J. Gao, F. Liu, Y. Liu, N. Ma, Z. Wang and X. Zhang, Environment-friendly method to produce graphene that employs vitamin C and amino acid, *Chem. Mater.* **22**, 2010, 2213–2218.

[42]
C.K. Chua and M. Pumera, The reduction of graphene oxide with hydrazine: elucidating its reductive capability based on a reaction-model approach, *Chem. Commun.* **52**, 2016, 72–75.

[43]
K.N. Kudin, B. Ozbas, H.C. Schniepp, R.K. Prud'homme, I.A. Aksay and R. Car, *Nano Lett.* **8**, 2008, 36.

[44]
P.S. Fernández, Modificación superficial de materiales de carbono: grafito y grafeno, 2011, Departamento de Ciencia de los Materiales e Ingeniería Metalúrgica. Universidad de Oviedo.

[45]
A.C. Ferrari and J. Robertson, Interpretation of Raman spectra of disordered and amorphous carbon, *Phys. Rev. B – Condens. Matter Mater. Phys.* **61**, 2000, 14095–14107.

[46]
M.M. Lucchese, F. Stavale, E.H.M. Ferreira, C. Vilani, M.V.O. Moutinho, R.B. Capaz, C.A. Achete and A. Jorio, Quantifying ion-induced defects and Raman relaxation length in graphene, *Carbon* **48**, 2010, 1592–1597.

Graphical abstract

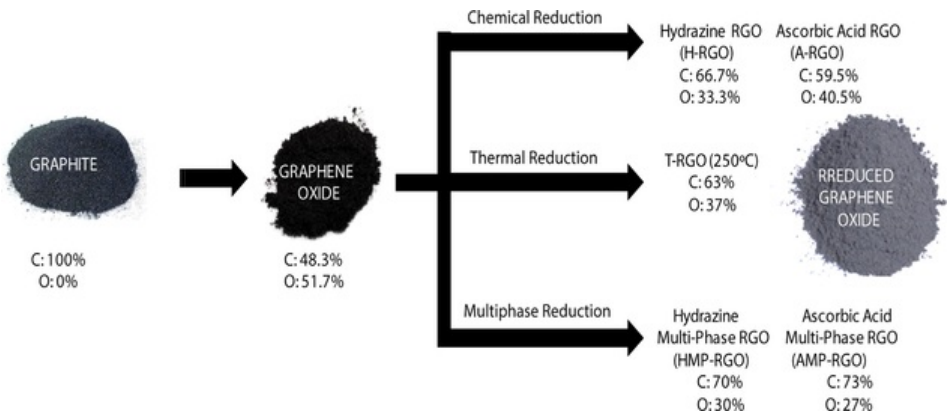

Highlights

- Chemical, thermal and multiphase strategies for the synthesis of RGO are proposed.
- Lowest amount of oxygen functional groups was obtained by multiphase reduction.
- Ascorbic Acid was presented as the best reduction agent in multiphase reduction.
- Multiphase reduction does not increase the number of defects in RGO structure.
- Structure and application of RGO highly depend on the reduction strategy followed.

Queries and Answers

Query: Your article is registered as a regular item and is being processed for inclusion in a regular issue of the journal. If this is NOT correct and your article belongs to a Special Issue/Collection please contact a.kurian@elsevier.com immediately prior to returning your corrections.
Answer: Yes, my article should be included in a regular issue.

Query: The author names have been tagged as given names and surnames (surnames are highlighted in teal color). Please confirm if they have been identified correctly.
Answer: Yes, the surnames have been identified correctly.

Query: Please check the hierarchy of the section headings.
Answer: Yes